

# Quantitative Performance Analysis of Hybrid Mesh Segmentation

Vaibhav J Hase<sup>1</sup>[0000-0002-5999-5175], Yogesh J Bhalerao<sup>2,3</sup>[0000-0002-0743-8633], Mahesh P Nagarkar<sup>4</sup>[0000-0002-1256-7552], and Sandip N Jadhav<sup>5</sup>[0000-0002-5544-0850]

<sup>1</sup> Amrutvahini College of Engineering, Department of Mechanical Engineering, Savitribai Phule Pune University, Sangamner, India

<sup>2</sup> Engineering, Faculty of Science, University of East Anglia, Norwich Research Park, Norwich NR47TJ, United Kingdom

[Y.bhalerao@uea.ac.uk](mailto:Y.bhalerao@uea.ac.uk)

<http://www.yogeshbhalerao.com>

<sup>3</sup> School of Mechanical Engineering, MIT Academy of Engineering, Alandi, Pune, India

[yogeshjbhalerao@gmail.com](mailto:yogeshjbhalerao@gmail.com)

<sup>4</sup> SCSM College of Engineering, Department of Mechanical Engineering, Savitribai Phule Pune University, Ahmednagar, India

[maheshnagarkar@rediffmail.com](mailto:maheshnagarkar@rediffmail.com)

<sup>5</sup> CEO (CAD), Centre for Computational Technologies (CCTech), Pune, India  
[sandip@cctech.co.in](mailto:sandip@cctech.co.in)

**Abstract.** This paper presents a comprehensive quantitative performance analysis of hybrid mesh segmentation algorithm. An important contribution of this proposed hybrid mesh segmentation algorithm is that it clusters facets using “facet area” as a novel mesh attribute. The method does not require to set any critical parameters for segmentation. The performance of the proposed algorithm is evaluated by comparing the proposed algorithm with the recently developed state-of-the-art algorithms in terms of coverage, time complexity, and accuracy. The experimentation results on various benchmark test cases demonstrate that Hybrid Mesh Segmentation approach does not depend on complex attributes, and outperforms the existing state-of-the-art algorithms. The simulation reveals that Hybrid Mesh Segmentation achieves a promising performance with coverage of more than 95%.

**Keywords:** CAD mesh model· Coverage· Feature recognition· Hybrid mesh segmentation· Interacting features.

## 1 Introduction

In today’s industrial perspective, automation of design and manufacturing activities poses many difficulties in seamless CAD-CAM integration. Almost all commercial CAD-CAM system used their proprietary file formats to store and

retrieval of feature data, which lead to interoperability and CAD-CAM integration problem.

Feature Recognition (FR) provides a communication medium between CAD and manufacturing application. FR manipulates geometrical data seamlessly from the CAD system to a CAM system or vice versa. FR is the first stage for seamless CAD-CAM integration. FR makes smart solid out of dumb solid. It acts as a bridge between CAD-CAM. However, FR technology is not mature enough, and platform dependent.

Standard Triangulated Language (STL) format is not much explored for CAM due to lack of feature recognition interface. Thus, a practical approach for FR from the CAD model is required, to work as an interface between CAD and CAM. Features from Computer-Aided Design (CAD) mesh models (CMM) can be employed to enhance mesh model, mesh simplification, and Finite Element Analysis (FEA).

Fully automatic manufacturing of mechanical parts, it is essential to recognize machining features such as complex interacting holes and blends, as they constitute a significant percentage of features in CMM[1]. The last four decades have witnessed significant research work in FR from B-rep models, while innovative manufacturing and design systems are mesh-based. Therefore, there's an urgent need to make smart solid out of dumb mesh model. Hence, this research work primarily aims at addressing this issue. The focus of the proposed work is to extract complex interacting features along with blends from the STL model. Furthermore, developing a fully automatic FR system from the CAD Mesh Model (CMM) is a challenging task.

Several mesh segmentation algorithms are available in the literature. As Scan Derived Mesh (SDM) have uniform tessellation throughout the mesh, segmentation methods of SDM cannot be applied to CMM [2]. The commonly utilized mesh attributes for mesh segmentation are curvature, convexity, dihedral angle, geodesic distance, etc.

Mesh segmentation is the most supported methodology for FR [3]. An elegant, unique, platform-independent hybrid mesh segmentation method has been developed, for the extraction of features from the CMM. The proposed method extracts intersecting features along with their parameters built over the segmentation workflow. The HMS algorithm also detects intersecting features and separates them.

This paper presents a comprehensive performance analysis of Hybrid Mesh Segmentation (HMS) algorithm quantitatively. The performance of the proposed algorithm is evaluated by comparing the proposed algorithm with the recently developed state-of-the-art algorithms like Attene et al. [4], RANSAC [5], Li et al. [6], Yan et al. [7], Adhikary and Gurumoorthy [8], and Le and Duan [9] in terms of coverage, time complexity, and accuracy. An important contribution of this proposed HMS is that it clusters facets using "facet area" as a novel mesh attribute. The method does not require to set any critical parameters for segmentation.

The rest of the paper is structured as follows: Section 2 provides a comprehensive review of relevant literature; Section 3 illustrates a proposed Hybrid mesh segmentation algorithm. Section 4 deals with the quantitative performance analysis of HMS. Discussion based on results is provided in Section 5. Section 6 present conclusion and future scope.

## 2 Literature Review

Mesh segmentation partition the input CMM into “meaningful” regions [7]. Over past four decades, several researches [3,9–15] have comprehensively summarized mesh segmentation methods with their strengths and weaknesses. Mesh attributes plays crucial role in success of segmentation results. Mesh segmentation is the most preferred approach for FR [3].

STL models of mechanical parts have sparse and dense triangles (see Figure 1(a) and Figure 2(a)). Flat surfaces have sparse and big triangles. Highly curved surfaces have dense and small triangles. Ruled surfaces have triangles of a small base [16,17]. Because of such a diverse variety of triangles in the STL model, computing the principal curvatures accurately is a tough task for coarse meshes [18]. Angelo et al. [19] presented a segmentation method to extract blend features using principal curvatures from a tessellated model. Features detected are fillets, rounds, and grooves. Conical surfaces were not detected.

Several scientists have tried to estimate curvature along the boundary [20]. Nevertheless, only the curvature knowledge (“Gaussian curvature” and “absolute mean curvature”) is not sufficient to identify sphere or cylinder alone. The curvature is also strongly influenced by non-uniformly and sparsely distributed facets [21]. It takes a lot of time to measure the curvature. Many mesh segmentation methods, when computing curvature, set a local threshold. It is difficult to establish a single global threshold [22–25]. Sunil and Pande [16] proposed a hybrid region-based segmentation system based on shape properties to identify freeform features from a tessellated sheet metal parts. This technique, however, can only be used to identify features that have a limited set of shape properties. When detecting complex parts, this method requires a user’s interaction. The method did not identify blends.

Research shows that triangle shape has more influence on discrete curvature than triangle size does [26]. There are very few researchers who use facets distribution properties of the STL for FR [27]. Hardly any of the algorithms took benefit of intrinsic surface properties of the facets distribution. This could be the first attempt, to take advantage of facets distribution for PM segmentation, and to extract various types of geometric primitives. Based on the quantitative relationship between mesh quality and discrete curvature [27], a HMS (vertex based + facet based + Artificial Neural Network (ANN)+and Rule-based techniques) have developed to partition CMM using “facet area”, avoiding tedious curvature estimation [28].

As the focus of this research paper to evaluate the performance of HMS by comparing with existing and recent state-of-the-art approaches, here, we limit our review of those approaches only.

Katz and Tal [29] proposed a “Hierarchical Mesh Decomposition using fuzzy clustering and cuts (HMD) method based on a fuzzy K-means iterative clustering algorithm.” However, the iterative clustering technique cannot be applied directly to segment mechanical parts [9]. Further, Katz et al. [30] presented a hierarchical mesh segmentation method using Feature Point and Core Extraction (FPCA). This method did not require information about the number of segments. However, the algorithm was iterative and reiterate until getting characteristic feature points like high convexities or concavities.

Mortara et al. [31] developed “Multi-Scale mesh Analysis by using the paradigm of Blowing Bubbles (MSABB)”. They segmented shape into clusters of vertices that have a uniform behavior from the point of view of the shape morphological feature characteristics. However, the method was curvature dependent.

Attene. et al. [4] developed the “Hierarchical Fitting Primitives” (HFP), a mesh segmentation framework that involves visual inspection along with a number of clusters as an input parameter. However, it is difficult to know a number of clusters before FR. Figure 1(b) and Figure 2(b) illustrates the failure cases of Attene et al.[4].

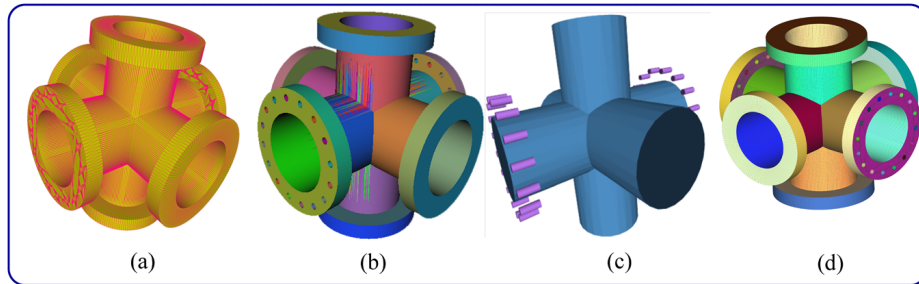


**Fig. 1.** Illustration of benchmark test cases failures a) Input CMM b) Attene et.al [4] c) Muraleedharan et al. [32] d) Output.

Schnabel et al. [5] developed a system for the identification of basic primitives based on “RANSAC (RANDOM Sample Consensus)”. This method over or under segment the model. Li et al. [6] invented the “GlobFit” method, which is a modified version of “RANSAC” [5] approach. Instead of segmentation, this approach is primitive fitting. For primitive extraction, they used parallel, orthogonal, equal angle relationships. This method is computationally more expensive and depends heavily on performance from “RANSAC” [5]. Yan et al. [7] developed “geometric distance-based error function” based mesh segmentation algorithm for the CMM or scanned model by fitting a general quadric surfaces. However, the technique was only suitable for the quadric surface. Not appropriate to blend detection.



Shapira et al. [33] presented a Gaussian distribution based part type mesh segmentation using “Shape Diameter Function (SDF)”. SDF provides a good distinction between thick and thin parts of the object. They clustered facets using “Gaussian Mixture Model (GMM)” which is sensitive to noise. However, SDF has its limitation on non-cylindrical parts of objects.

Adhikary and Gurumoorthy [8] had developed “Minimum Feature Dimension (MFD)” based free-form volumetric features extraction technique. They identified feature boundary edges from CMM by 2D slicing, without segmentation. The algorithm does not rely on mesh triangle density, and mesh geometrical properties. However, for the test case shown in Figure 2(a), the algorithm was unable to detect and extract features. MBD must be known prior to extraction of the feature. Figure 2(c) illustrates the failure case of Adhikary and Gurumoorthy [8].

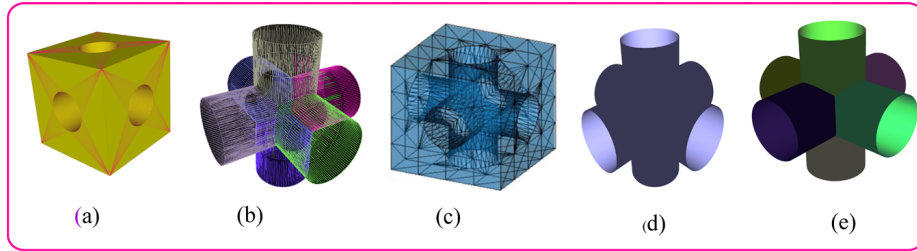


**Fig. 2.** Illustration of benchmark test cases failures a) Input CMM b) Attene et.al [4] c) Adhikary and Gurumoorthy [8] d) Muraleedharan et al. [32] e) Output.

Le and Duan [9] proposed a “dimensional reduction technique” in which profile curve analysis has been carried out. To obtain a profile curve, they transform 3D primitives into 2D. However, the algorithm was dependent on slice thickness, and slicing techniques fail to detect or separate complex interacting features as noted by [8].

Volumetric interacting features were recognized by Muraleedharan et al. [32] using “a random cutting plane technique”. They utilized “Gaussian curvature” for boundary detection and separating the interacting features. However, their algorithm relies on “number of cutting planes” for FR which must be known prior to extraction. The feature must have an inner ring presence, which is the algorithm’s key weakness. If there were no inner rings (for a joint have complex boundary) in a feature, it remained undetected. The failure case of Muraleedharan et al. [32]. is illustrated in Figure 1(c) and Figure 2(d).

HMS extracts and separates intersecting features. Figure 1(d) and Figure 2(e) shows success of HMS in feature recognition.

### 3 Hybrid Mesh Segmentation

HMS automatically segment CMM into “meaningful” and distinct, mathematically analyzable analytic regions [7,21]

#### 3.1 Architectural Framework of Hybrid mesh segmentation

Figure 3 illustrates an architectural framework of HMS. It includes three stages viz. pre-processing, mesh segmentation, and iterative region merging.

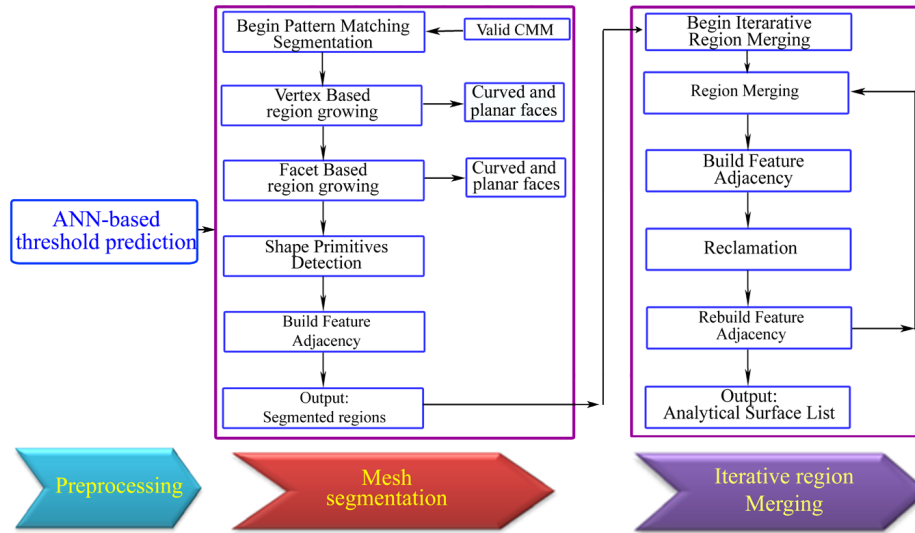


**Fig. 3.** Illustrates a Architectural Framework of Hybrid mesh segmentation.

**Preprocessing** Topology and facet adjacency are constructed in imported CMM, and automated threshold prediction has been performed.

*Input CAD Mesh Model* The HMS takes a valid CMM which is free from errors as input in ASCII or Binary format, therefore, there is no need for model healing [16].

*Automatic Threshold Prediction* Segmentation of CMM leads to under segmentation or over-segmentation based on input Area Deviation Factor ( $Adf$ ) [12,32]. Setting the appropriate  $Adf$  is too complicated for a layman. Therefore, an automatic prediction of  $Adf$  is of great importance. Hase et al. [34] proposes and implements smart prediction of  $Adf$  using the Artificial Neural Network (ANN). A detailed description is beyond this paper’s reach.

**Mesh segmentation** Segmenting CMM is difficult by using a stand-alone vertex-based (*VBRG*) or facet based region growing (*FBRG*) techniques [31]. A promising approach that has become evident is a hybrid (*VBRG* + *FBRG*) one, wherein the advantages of the above approaches are combined.

HMS utilizes the “facet area” as an attribute for segmenting CMM. It combines *VBRG* and *FBRG* algorithms. HMS automatically segments CMM into meaningful analytic surfaces without curvature estimation.

**Iterative region merging** Iterative region merging repeatedly merged over segmented regions that have similar geometric property to generate a single region. It includes following steps:

*Region Merging* Region merging merge regions iteratively. It’s not enough to combine all regions with a single pass. Two adjacent regions are merge to one, if they satisfy *geometry equality test*. Region adjacency may have changed after merging, so in the next iteration, features that were not eligible for merging in the previous iteration, will be merged.

*Reclamation* After region merging, small cracks may found at the region boundaries [35]. To make a watertight model, uncollected facets were reclaimed into the specified surrounding region, based on *reclamation criteria*.

For further implementation details of HMS, please refer to [36,37].

### 3.2 Illustrative examples

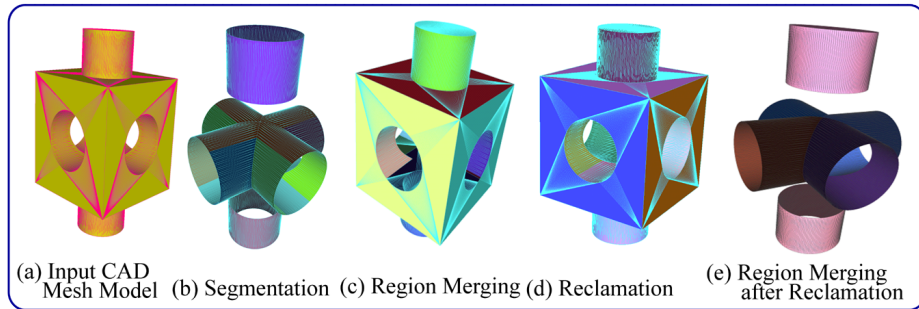


**Fig. 4.** Illustrates the hybrid mesh segmentation process.

Figure 4(a) to 4(e) briefly illustrates all stages in hybrid mesh segmentation for the STL CAD mesh model. Experimental evaluation is carried out on the “Box” model. The part is created in Autodesk<sup>TM</sup> Inventor<sup>TM</sup> 2018 and has been exported as a CMM. This part is used to test the efficacy of the proposed algorithm wherein cylindrical features intersect with one another forming complex

boundaries at the intersections. Table 1 outline the parameters for the “Box” model. Table 2 outlines primitives detected before merging and after merging. The system takes 0.31 seconds for segmentation. Table 3 shows the performance of *HMS* with detailed timings for each step.

**Table 1.** Outline the parameters for the Box model.

<i>Particulars</i>	<i>Descriptions</i>
Vertex Count	1390
Facet Count	2788
Area Deviation Factor	0.75
Sharp Edge Angle	40°
Dihedral Angle	40°
Coverage	100%

**Table 2.** Illustrates the region merging process.

<i>Feature</i>	<i>Before merging</i>	<i>After merging</i>
Planes	8	80
Cylinder	10	6
<b>Overall time elapsed</b>		<b>0.31s</b>

**Table 3.** Timings statistics for the “Box” model.

<i>Particulars</i>	<i>Time elapsed in seconds</i>
Mesh import and topology generation	0.08
Planar face segmentation	0.043
Curved face segmentation	0.063
Region merging	0.003
Reclamation	0.012
Iterative region merging	0.011
<b>Overall: Time elapsed</b>	<b>0.31</b>

## 4 Quantitative Performance Analysis of HMS

The output of HMS algorithm quantitatively assessed by performing simulation on benchmark test cases using a computer with windows 8.1 operating system, and with Intel Core i3 processor.

### 4.1 Quantitative Performance Measure

The quantitative performance measure used in the investigation are:

**Coverage** The success of the method quantified by coverage assessment. The percentage coverage is used as a measure of an indicator of the successful segmentation algorithm. The coverage is calculated as:

$$Coverage = \frac{Number\ of\ primitives\ extracted}{Actual\ number\ of\ primitives\ present} \quad (1)$$

**Absolute Distance error** An absolute error is found by comparing parameters of recovered features with a standard reference.

$$Distance\ Error = |Measured\ Distance - Actual\ Distance| \quad (2)$$

**Time** The overall time (in seconds) needed for various steps of mesh segmentation are:

- Step 1: Mesh import and topology generation
- Step 2: Hybrid mesh segmentation
- Step 3: Building feature adjacency
- Step 4: Region merging
- Step 5: Reclamation
- Step 6: Iterative region merging
- Step 7: Feature recognition

**Number of regions before/after region merging** Iterative region merging technique merges a number of regions before merging ( $N_{Rbrm}$ ) to a single region that has a similar geometric property ( $N_{Rarm}$  : number of regions after region merging).

## 4.2 Evaluation of Segmentation Algorithms

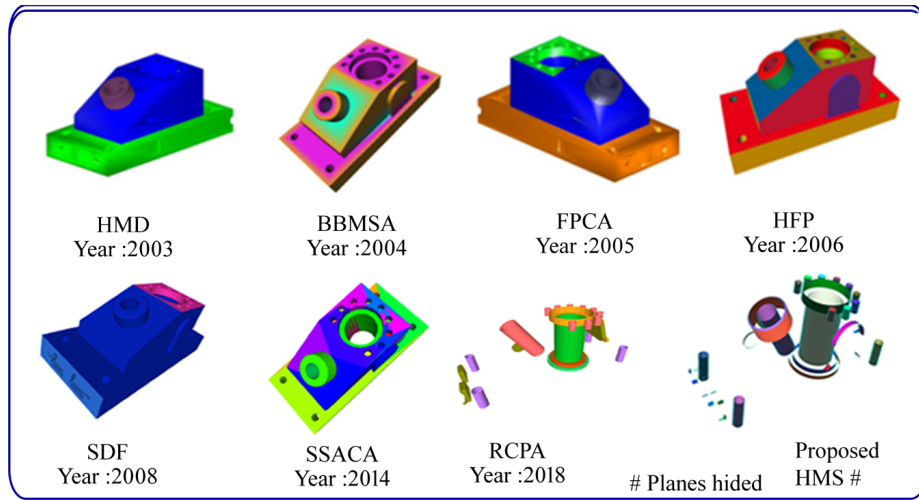
The efficacy of the proposed algorithm was tested by comparing with the existing state-of-art approaches. Table 4 shows the existing state of art approaches. The proposed algorithm has been tested on benchmark “Anchor” model with different approaches, as shown in Figure 5. For SDF [33], SSACA [38], and HFP [4] approach for which the code was publicly available. For methods BBMSA [31], HMD [29], FPCA [30], and RCPA [32] are taken from [11] [32] as the code was not publically available. The HMS approach extracted all the features with coverage (C) of 100%. Comparing with the existing state-of-the-art approaches, the closest one among others is the technique HFP of Attene et al. [4]. Others existing approaches under segments the model, making feature extraction a difficult task. Table 5 evaluates the time performance of the proposed algorithm for the test cases shown in Figure 6.

## 4.3 Comparison with the recently developed algorithm

The experimentation results on various benchmark test cases demonstrate that, HMS approach does not depend on complex attributes, and outperforms the

**Table 4.** Existing state-of-the-art approaches.

<i>Authors/ Reference</i>	<i>Year</i>	<i>Methodology</i>	<i>Code Availability</i>	<i>Abbreviation</i>
Katz and Tal [29]	2003	“Hierarchical mesh decomposition using Fuzzy Clustering.”	No	HMD
Mortara et al. [31]	2004	“Blowing Bubbles for Multi-Scale Analysis”	No	BBMSA
Katz et al. [30]	2005	“Mesh segmentation using feature point and core extraction.”	No	FPCA
Attene et al.[4]	2006	“Hierarchical mesh segmentation based on fitting primitives.”	Yes	HFP
Shapira et al. [33]	2008	“Mesh segmentation using shape diameter function.”	Yes	SDF
Kaick et al. [38]	2014	“Shape Segmentation by Approximate Convexity Analysis”	Yes	SSACA
Muraleedharan et al. [32]	2018	“Random cutting plane approach.”	No	RCPA
<b>Hase et al. [36]</b>	<b>2019</b>	<b>“Hybrid Mesh segmentation”</b>	<b>Yes</b>	<b>HMS</b>

**Fig. 5.** Performance comparisons of the proposed method with existing approaches on benchmark “Anchor” model.

**Table 5.** Qualitative performance analysis of existing state-of-the-art approaches.

<i>Test Cases</i>	<i>F</i>	<i>V</i>	<i>S</i>	<i>Adf</i>	<i>N<sub>Rbrm</sub></i>	<i>N<sub>Rarm</sub></i>	<i>T</i>
Optics housing	1182	593	0.306	0.75	49	35	0.186
Demo08	2492	1238	0.644	0.75	82	32	0.289
Cami1	944	464	0.246	0.70	36	18	0.18
Caddy02	1644	822	0.43	0.75	30	18	0.268
Gear_38	2696	1340	0.681	0.75	26	23	0.36

Wherein, *F*: Number of Facets *V*: Number of Vertex *S*: STL Size (in MB)  
*Adf*: Predicted Area deviation factor  
*T*: Overall Timing (in a second)

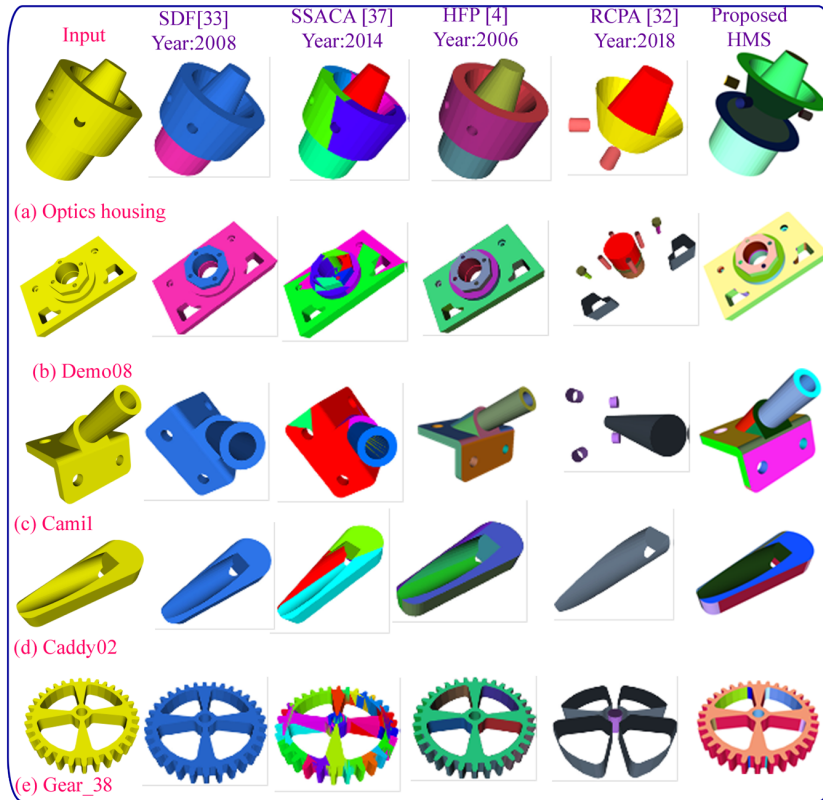


**Fig. 6.** Comparison of volumetric and surface-based FR with existing approaches.

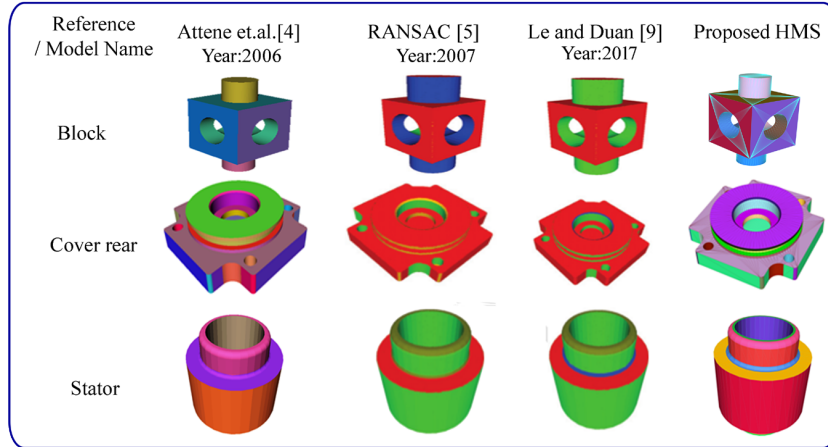


Fig. 7. Comparison with the existing algorithms [39].

existing state-of-the-art algorithms. Table 6 summarizes the quantitative comparison of HMS for the test cases. We evaluate using the coverage percentage, a number of primitives, and the distance error. As noted by [39], the HMS algorithm yields better results than RANSAC [5] and Attene et al. [4]. (see Fig.7). HMS results are comparable to Le and Duan [9]. The simulation reveals that HMS achieves a promising performance with coverage of more than 95%.

Table 6. Quantitative evaluation of primitive quality in Figure 7.

Model Name	# of Primitives					Coverage (%)					Distance Error ( $\times 10^{-3}$ )				
	I	II	III	IV	V	I	II	III	IV	V	I	II	III	IV	V
Block	14	14	14	9	14	100	99.98	99.98	64.28	98.98	0.04	0.37	0.08	n/a	0.69
Cover rear	45	28	45	45	28	100	87.79	100	100	87.79	0.02	0.11	0.04	n/a	0.15
Stator	12	12	12	6	n/a	100	99.99	100	50	n/a	0.01	0.8	0.47	n/a	n/a

(I) Proposed algorithm (II) RANSAC [5] (III) Le and Duan [9] (IV) Attene et al. [4] (V) GlobFit et al. [6]

## 5 Results and Discussions

### 5.1 Evaluation of Segmentation Results

As noted by Adhikary and Gurumoorthy [8], it is challenging to extract interacting features. The algorithm developed by Muraleedharan et al. [32] is unable to separate the interacting features as these models do not have a presence of inner rings. Most of the existing algorithms pose difficulties in extracting and separating interacting features as joints between them have complex boundaries. The



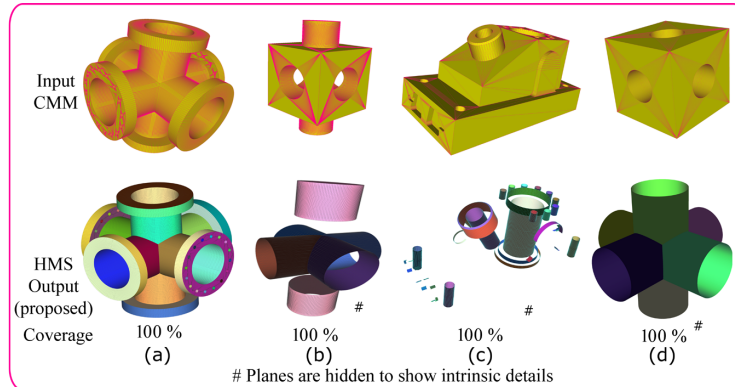


**Fig. 8.** Experimental results for proposed HMS.

HMS algorithm extract and separate interacting features. The HMS algorithm requires no prior knowledge of attributes like “the number of clusters”, “curvature”, “the number of cutting planes”, “minimum feature dimension”, “the orientation of model”, and “thickness of the slice” to extract volumetric features. Figures 8(a) to 8(d) briefly illustrates the results of the HMS algorithm for extracting interacting features. Table 7 shows experimental results for different CMM as shown in Figures 8.

**Table 7.** Experimental results for different CMM shown in Figures 8.

<i>Test Cases</i>	<i>F</i>	<i>V</i>	<i>S</i>	<i>Adf</i>	<i>N<sub>Rbm</sub></i>	<i>N<sub>Rarm</sub></i>	<i>T</i>	<i>C</i>
Figure 8(a)	17104	8480	2.931	0.65	537	62	2.52	100
Figure 8(b)	2788	1390	0.709	0.60	18	14	0.816	100
Figure 8(c)	7100	3542	1.837	0.75	210	80	0.927	100
Figure 8(d)	3360	1672	0.875	0.60	117	12	0.375	100

## 5.2 Error Analysis

A quantitative analysis of HMS is performed. Figure 9(a) illustrates an input CMM with parameters to do quantitative analysis. All features parameters have selected as a standard reference for comparison. After FR, features parameters are recovered.

An absolute error is found by comparing parameters of recovered features with a standard reference. A quantitative error analysis of HMS algorithm in the extraction of the feature parameter shows that recovered values are very close to those of the input CAD model, as shown in Table 8.

**Table 8.** A quantitative error analysis in the extraction of the feature parameter.

Feature	Checked Values	Value Got from CMM	Value Got by Mesh FR	Absolute Error
Cylinder_F1	Axis	(0,1,0)	(-0.000000, 1.000000, 0.000000)	0
	Radius	10	10	0
	Axis point	(0,0,0)	(0.000000, 0.000000, -0.000000)	0
	End point1	(0, 29.71, 0)	(0.000000, 29.707320, -0.000000)	0
	End point2	(0, 43.71, 0)	(0.000000, 43.707320, 0.000000)	0
Cylinder_F2	Axis	(0,1,0)	(0.000000, 1.000000, 0.000000)	0
	Radius	15	15	0
	Axis point	(0,0,0)	(-0.000000, 0.000000, -0.000000)	0
	End point1	(0, 16.71, 0)	(-0.000000, 16.707320, -0.000000)	0
	End point2	(0, 26.71, 0)	(-0.000000, 26.707320, -0.000000)	0
Cylinder_F3	Axis	(0,1,0)	(-0.000001, 1.000000, 0.000000)	0
	Radius	25	25	0
	Axis point	(0,0,0)	(0.000032, 0.000000, -0.000004)	0
	End point1	(0, 48.71, 0)	(0.000002, 48.707304, -0.000001)	0
	End point2	(0, 56.71, 0)	(-0.000003, 56.707336, 0.000000)	0
Sphere_V1	Center	(0, 2.16, 0)	(-0.000330, 2.161758, 0.000490)	0
	Radius	60	60.0021	0.0021
Sphere_V4	Center	(0, 3.17, 0)	(0.000003, 3.166820, -0.000007)	0
	Radius	2.12	2.11565	0.00435
Cone_F5	Apex point	(0, 23.71, 0)	(0.000000, 23.707310, -0.000000)	0
	Axis	(0,-1,0)	(0.000000, -1.000000, 0.000000)	0
	Angle	0.79	0.785398	0.004602
	Major centre	(0, 48.71, 0)	(-0.000000, 48.707320, -0.000001)	0
	Minor centre	(0, 46.71, 0)	(0.000000, 46.707320, -0.000000)	0
Cone_F7	Apex point	(0,0,0)	(-0.000000, 0.000000, 0.000005)	0
	Axis	(0,1,0)	(0.000000, 1.000000, -0.000003)	0
	Angle	0.73	0.731604	0.001604
	Major centre	(0, 16.71, 0)	(-0.000000, 16.707317, -0.000000)	0
	Minor centre	(0, 1.75, 0)	(-0.000000, 1.753428, 0.000000)	0
Torus_v2	Axis	(0,-1,0)	(-0.000000, -1.000000, -0.000000)	0
	Center	(0, 29.71, 0)	(0.000070, 29.707337, 0.000070)	0
	Major radius	13	12.9999	0.0001
	Minor radius	3	3.00004	0.0004
Torus_v3	Axis	(0,1,0)	(0.000000, 1.000000, 0.000000)	0
	Center	(0,43.71,0)	(-0.002234, 43.707458, 0.000000)	0
	Major radius	13	13.0021	0.0021
	Minor radius	3	2.99983	0.00017

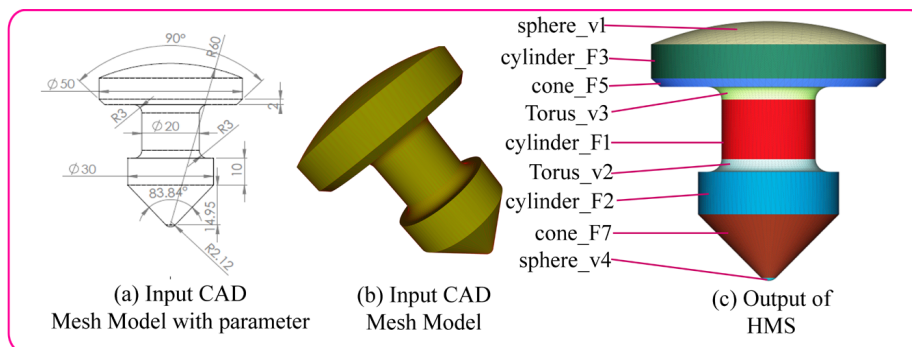


**Fig. 9.** A quantitative analysis of HMS.

### 5.3 Mesh Density

The HMS algorithm has been tested with varying mesh density. As different solid modeler has its own techniques of generating a tessellated model, results in each model have varying mesh density, mesh pattern, and mesh quality. Based on mesh quality, ANN predicts the area deviation factor automatically [34]. Experiments show that the HMS algorithm has no difficulty in extracting the features correctly. The system identifies seven planer, eight cylindrical, one conical, and three-torus surfaces. Also, primitive parameters are estimated accurately. Table 9 shows the details of the “Assy” model shown in Figure 10.

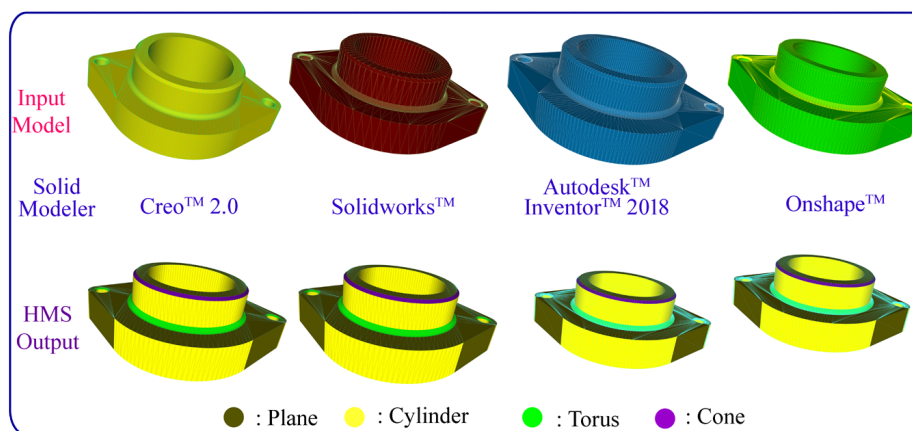


**Fig. 10.** Experimental results for “Assy” model.

**Table 9.** Experimental results for “Assy” model with varying mesh density.

<i>Test Cases</i>	<i>F</i>	<i>V</i>	<i>S</i>	<i>Adf</i>	<i>N<sub>Rbrm</sub></i>	<i>N<sub>Rarm</sub></i>	<i>T</i>	<i>Solid Modeler</i>	<i>C</i>
Assy	5628	2810	1.41	0.8261	43	19	0.605	Creo <sup>TM</sup> 2.0	100
Assy	7172	3582	1.96	0.75	105	19	0.727	Solidworks <sup>TM</sup> 2017	100
Assy	8022	4007	2.03	0.8	65	19	0.813	Autodesk <sup>TM</sup> Inventor <sup>TM</sup> 2018	100
Assy	34304	17148	6.42	0.75	30	19	2.914	Onshape <sup>TM</sup>	100

#### 5.4 Discussions

**Efficacy Measure of Hybrid Mesh Segmentation** The experimentation results on three case studies demonstrate that HMS algorithm extract and separate interacting features. Results are tabulated in Table 10 and presented in the bar charts, refer Figure 11 to Figure 13.

From Table 10 and Figure 11, it is observed that the stand-alone vertex-based region growing (**VBRG**) able to extract planer (**P**) surface successfully for all three test cases (see Figure 14(b), 17(b), 20(b)) and unable to detect curved (**C**) surface (undetected or miss out surfaces). For the test case “Box”, **VBRG** detect 8 planer surface, and 6 curved surfaces which are undetected, see Figure 14(d).

**Table 10.** Quantitative evaluation of primitive quality for test cases.

<i>Model Name</i>	<i>F</i>	<i>V</i>	<i>S</i>	<i>Adf</i>	<i>Number of Primitives</i>						<i>Coverage (%)</i>			<i>Overall Timing(s)</i>		
					<i>VBRG</i>		<i>FBRG</i>		<i>HMS</i>		<i>VBRG</i>	<i>FBRG</i>	<i>HMS</i>	<i>VBRG</i>	<i>FBRG</i>	<i>HMS</i>
					<i>P</i>	<i>C</i>	<i>P</i>	<i>C</i>	<i>P</i>	<i>C</i>						
Box	2788	1390	0.709	0.60	8	0	8	2	8	6	57.14	71.43	<b>100</b>	0.402	5.239	<b>0.368</b>
Stator	2592	1296	0.665	0.75	4	4	4	8	4	8	66.67	100	<b>100</b>	0.37	0.463	<b>0.396</b>
Pipe	17104	8480	2.87	0.65	12	0	12	50	12	50	19.35	100	<b>100</b>	1.97	2.99	<b>2.52</b>

For the test case “Stator” **VBRG** detect 4 planer surface, 4 curved surfaces and 4 are undetected surfaces, see Figure 17(d). For the test case “Pipe” **VBRG** detect 12 planer surface, and 50 curved surfaces which are undetected, see Figure 20(d).

The stand-alone facet based region growing (**FBRG**) able to extract planer (**P**) and curved (**C**) surface fully or partially for all three test cases. For the test case “Box” **FBRG** detects 8 planer surface, 2 curved surfaces, and 4 undetected curved surfaces, see Figure 15(d). For the test case “Stator” **FBRG** detects 4 planer surface, 8 curved surfaces, and zero undetected curved surfaces, see Figure 18(d). For the test case “Pipe” **FBRG** detect 12 planer surfaces, 50 curved surfaces, and zero undetected curved surfaces, see Figure 21(d).

To measure the performance of HMS, coverage for **VBRG**, **FBRG**, and **HMS** computed. From Table 10 and Figure 12, it is observed that percentage coverage for all three test cases is 100% for **HMS**.

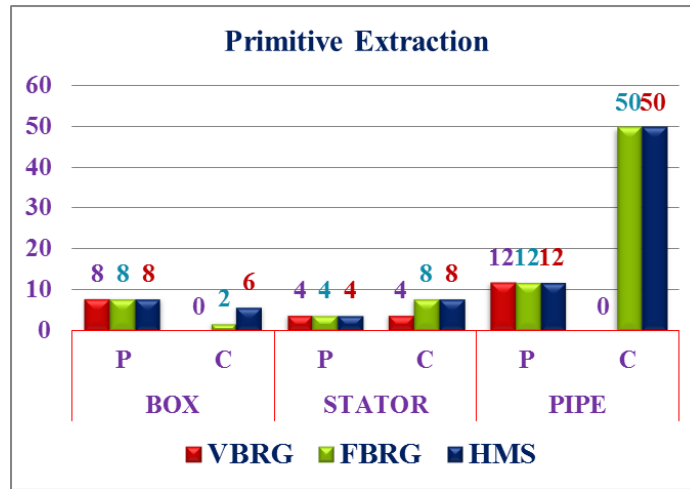


Fig. 11. Performance evaluation of HMS: Primitive Extraction.

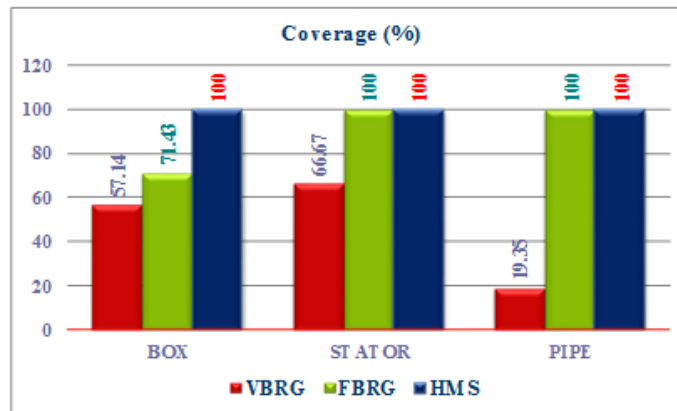


Fig. 12. Performance evaluation of HMS: Coverage.

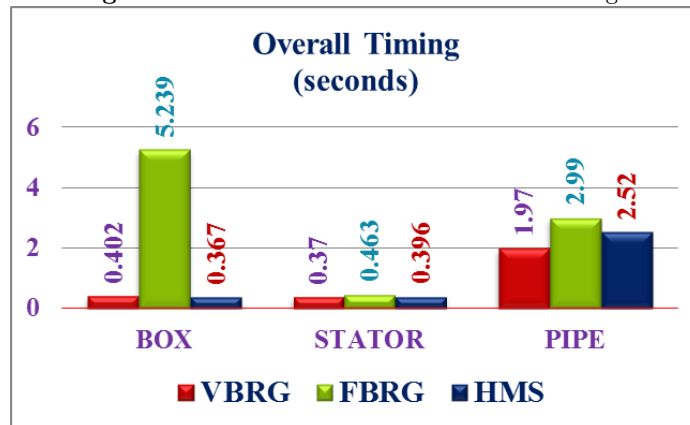


Fig. 13. Performance evaluation of HMS: Overall timing.

To evaluate the efficacy of the proposed technique, the overall timing for **VBRG**, **FBRG**, and **HMS** computed.

From Table 10 and Figure 13, it is observed that the overall timing needed for **HMS** is least as compared to stand-alone **VBRG** and **FBRG**. This is due to **HMS**, wherein an intelligent blending of **VBRG** and **FBRG** carried out.

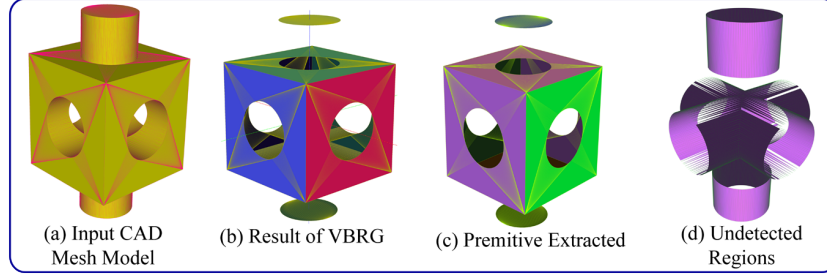


Fig. 14. Vertex based region growing (VBRG): Box model.

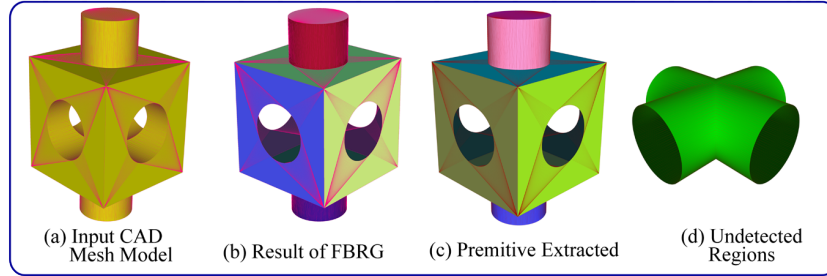


Fig. 15. Facet-based region growing (FBRG): Box model.

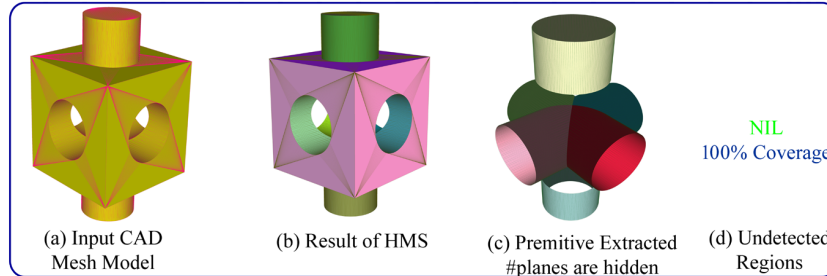


Fig. 16. Proposed hybrid mesh segmentation: Box model.

**Significance of Area Deviation Factor** The accuracy and reliability of HMS depend on *Adf*. Inadequate *Adf* leads to under segmentation or over-segmentation based on input. The small value of  $Adf < 0.60$  over segment the model whereas  $Adf > 0.80$  leads to under segment. Iterative region merging technique merges over

segmented regions to the similar adjacent region, results in increased the overall time of FR. Under-segmentation leads to inaccuracy. The proposed artificial neural networks (ANN) based predictor set optimum, i.e. (greater than 0.60 and less than 0.80) which results in better segmentation.

**Accuracy of FR** The prerequisite step for FR from the CMM is hybrid mesh segmentation. If the algorithm fails at the segmentation stage, leads to failure of FR. The whole segmentation process must be successfully accomplished for better accuracy of FR.

**Interacting Feature Recognition** The crucial problem for seamless CAD-CAM integration is interacting feature recognition. As features interact, their topology changes, and make it challenging to recognize resulting geometry. As previously stated (see Figure 1 and Figure 2), the existing techniques unable to separate the interacting features, HMS algorithm extract and separate interacting features along with the geometric parameter.

**Comparison of Techniques** The pertinent literature concerns with feature extraction with attributes like “the number of clusters”, “curvature”, “the number of cutting planes”, “minimum feature dimension”, “the orientation of model”, and “thickness of the slice” to extract features. The HMS technique is independent of these attributes.

Compared to the current state-of-the-art methods, perhaps the nearest one among others is Le and Duan’s method [9 ].

**Time Complexity** In this section, the computational complexity of the proposed algorithm is computed. A CAD Mesh Model consists of an ordered set of vertices  $S = \{v_i\}_i \subset R^3$  and a set of faces  $F = \{f_k = \Delta(v_{k1}, v_{k2}, v_{k3}, n_x, n_y, n_z)\}$   $S = \{V, F\}$

Let  $v \in V$  be a vertex of a,  $\mathbf{M}$ .  $T = \{t_1, t_2, \dots, t_k\}$  is the set of all triangles. For  $N_f$  and  $N_v$  denote the number of facets and the number of vertices, respectively of  $\mathbf{M}$ .  $A_m$  and  $N_m$  are the area and the normal vector of  $f_k$ .

Let the number of facets in the model is  $F$ , and the number of vertices in the model is  $V$ . In the region growing stage, the complexity of curved facets segmentation is  $O(V)$  using vertex based clustering and  $O(F)$  using facet based clustering. Let  $S_V$  be the number of curved facets. Planar face segmentation is run on the remaining facets, the complexity of which is  $O(F - S_V)$ . Let  $N_T$  be the number of features of a specific type (for, e.g., cylinder) detected after the region growing. Then the complexity of the region growing for that feature type is  $O(N_T)$ . Let  $K$  be the total number of features after the region merging step. Let  $P$  be the number of undetected facets after the region growing step. The complexity of iterative reclamation algorithm for  $P$  undetected facets with a single feature is  $O(P^2)$ . With  $K$  features, the complexity is  $O(K * P^2)$ .

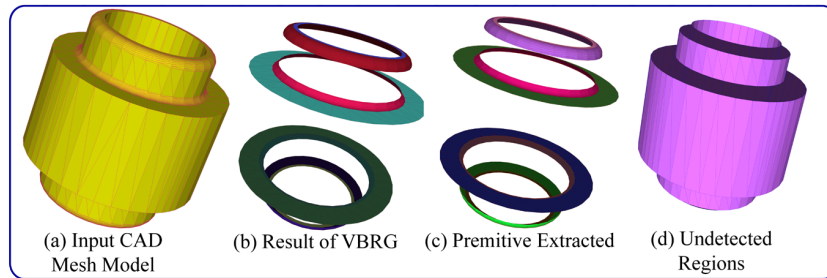


Fig. 17. Vertex based region growing (VBRG): Stator model.

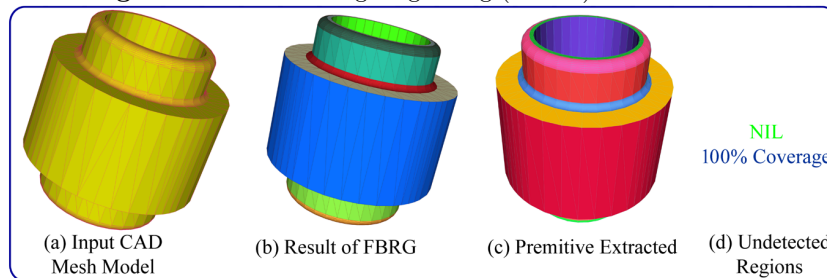


Fig. 18. Facet-based region growing (FBRG): Stator model.

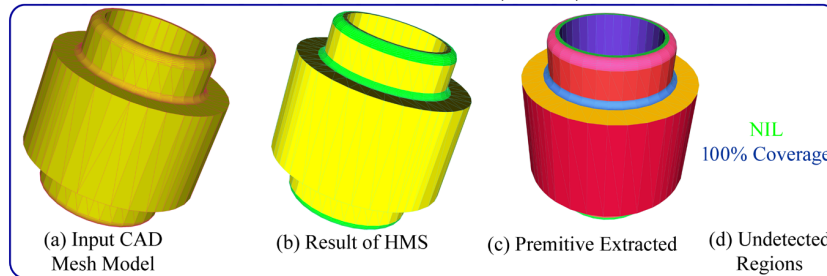


Fig. 19. Proposed hybrid mesh segmentation: Stator model.

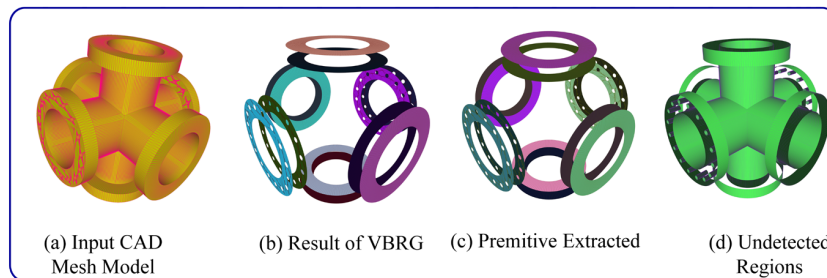
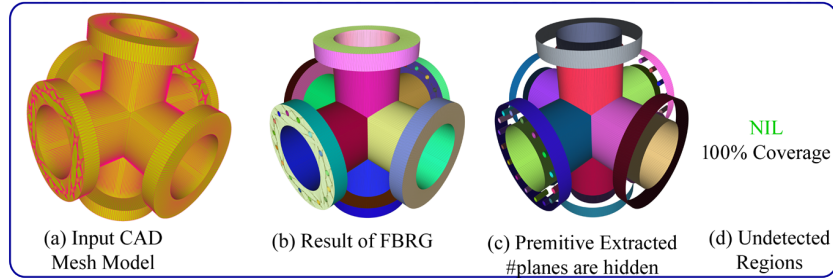
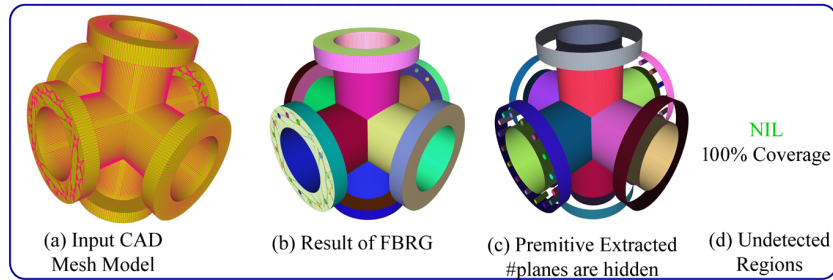


Fig. 20. Vertex based region growing (VBRG): Pipe model.





**Fig. 21.** Facet-based region growing (FBRG): Pipe model.



**Fig. 22.** Proposed hybrid mesh segmentation: Pipe model.

The performance of the proposed algorithm depends on the complexity of the model rather than its size. However, the maximum time is spent on mesh import and topology generation, and it depends on mesh size. The maximum time is spent on the curve and planer region segmentation whereas region merging takes the least time. Table 7 and Table 9 shows that the overall timing grows stiffly with varying in the number of facets.

## 6 Conclusion

In this paper, the performance of a hybrid segmentation algorithm has been quantitatively evaluated. The performance evaluated by comparing the proposed algorithm with the recently developed state-of-the-art algorithms, the effect of varying mesh density and mesh quality, and error analysis of HMS in the extraction of the feature parameter. The significance of Area Deviation Factor, the accuracy of FR, time complexity is also discussed.

The experimentation indicates that HMS outperforms the existing state-of-the-art algorithms and achieves a promising performance. The quantitative results proved that HMS algorithm is efficient and competent, and found to be robust and consistent with coverage of more than 95%.

Future research work will be carried out in the direction of deep learning-based FR. One may develop boundary representation (B-rep) model by segmenting CMM using HMS.

**Acknowledgments** This research was supported by Centre for Computational Technologies (CCTech), Pune, India. Special thanks are given to Dr. Truc Le and Dr. Ye Duan [9] for helping us to quantify percentage coverage. The authors are grateful to the authors Attene et.al. [4], RANSAC [5], and GlobFit et. al. [6] who have made their code available to the public.

## References

1. Raffbakhsh, N., Campbell, M.I.: Hierarchical Fuzzy Primitive Surface Classification From Tessellated Solids for Defining Part-to-Part Removal Directions. *J Comput Inf Sci Eng.* 18, 011006 (2017). <https://doi.org/10.1115/1.4038144>
2. Gao, S., Zhao, W., Lin, H., Yang, F., Chen, X.: Feature suppression based CAD mesh model simplification. *Comput Des.* 42, 1178–1188 (2010). <https://doi.org/10.1016/j.cad.2010.05.010>
3. Wang, J., Yu, Z.: Surface feature based mesh segmentation. *Comput Graph.* 35, 661–667 (2011). <https://doi.org/10.1016/j.cag.2011.03.016>
4. Attene, M., Falcidieno, B., Spagnuolo, M.: Hierarchical mesh segmentation based on fitting primitives. *Vis Comput.* 22, 181–193 (2006). <https://doi.org/10.1007/s00371-006-0375-x>
5. Schnabel, R., Wahl, R., Klein, R.: Efficient RANSAC for Point-Cloud Shape Detection. *Comput Graph Forum.* 26, 214–226 (2007). <https://doi.org/10.1111/j.1467-8659.2007.01016.x>
6. Li, Y., Wu, X., Chrysathou, Y., Sharf, A., Cohen-Or, D., Mitra, N.J.: GlobFit: Consistently Fitting Primitives by Discovering Global Relations. In: *ACM SIGGRAPH 2011 papers on - SIGGRAPH '11*. p. 1. ACM Press, New York, New York, USA (2011)
7. Yan, D.-M., Wang, W., Liu, Y., Yang, Z.: Variational mesh segmentation via quadric surface fitting. *Comput Des.* 44, 1072–1082 (2012). <https://doi.org/10.1016/j.cad.2012.04.005>
8. Adhikary, N., Gurumoorthy, B.: A slice based approach to recognize and extract free-form volumetric features in a CAD mesh model. *Comput Aided Des Appl.* 13, 587–599 (2016). <https://doi.org/10.1080/16864360.2016.1150703>
9. Le, T., Duan, Y.: A primitive-based 3D segmentation algorithm for mechanical CAD models. *Comput Aided Geom Des.* 52–53, 231–246 (2017). <https://doi.org/10.1016/j.cagd.2017.02.009>
10. Shamir, A.: A formulation of boundary mesh segmentation. In: *Proceedings. 2nd International Symposium on 3D Data Processing, Visualization and Transmission, 2004. 3DPVT 2004*. pp. 82–89. IEEE (2004). <https://doi.org/10.1109/TDPVT.2004.1335163>
11. Attene, M., Katz, S., Mortara, M., Patane, G., Spagnuolo, M., Tal, A.: Mesh Segmentation - A Comparative Study. In: *IEEE International Conference on Shape Modeling and Applications 2006 (SMI'06)*. pp. 7–7. IEEE (2006). <https://doi.org/10.1109/SMI.2006.24>

12. Agathos, A., Pratikakis, I., Perantonis, S., Sapidis, N., Azariadis, P.: 3D Mesh Segmentation Methodologies for CAD applications. *Comput Aided Des Appl.* 4, 827–841 (2007). <https://doi.org/10.1080/16864360.2007.10738515>
13. Shamir, A.: A survey on Mesh Segmentation Techniques. *Comput Graph Forum.* 27, 1539–1556 (2008). <https://doi.org/10.1111/j.1467-8659.2007.01103.x>
14. Chen, X., Golovinskiy, A., Funkhouser, T.: A benchmark for 3D mesh segmentation. *ACM Trans Graph.* 28,1 (2009). <https://doi.org/10.1145/1531326.1531379>
15. Theologou, P., Pratikakis, I., Theoharis, T.: A comprehensive overview of methodologies and performance evaluation frameworks in 3D mesh segmentation. *Comput Vis Image Underst.* 135, 49–82 (2015). <https://doi.org/10.1016/j.cviu.2014.12.008>
16. Sunil, V.B., Pande, S.S.: Automatic recognition of features from freeform surface CAD models. *Comput Des.* 40, 502–517 (2008). <https://doi.org/10.1016/j.cad.2008.01.006>
17. Xiao, D., Lin, H., Xian, C., Gao, S.: CAD mesh model segmentation by clustering. *Comput Graph.* 35, 685–691 (2011). <https://doi.org/10.1016/j.cag.2011.03.020>
18. Jiao, X., Bayyana, N.R.: Identification of and discontinuities for surface meshes in CAD. *Comput Des.* 40, 160–175 (2008). <https://doi.org/10.1016/j.cad.2007.10.005>
19. Di Angelo, L., Di Stefano, P., Morabito, A.E.: Secondary features segmentation from high-density tessellated surfaces. *Int J Interact Des Manuf.* 12, 801–809 (2018). <https://doi.org/10.1007/s12008-017-0426-8>
20. Razdan, A., Bae, M.: A hybrid approach to feature segmentation of triangle meshes. *Comput Des.* 35, 783–789 (2003). [https://doi.org/10.1016/S0010-4485\(02\)00101-X](https://doi.org/10.1016/S0010-4485(02)00101-X)
21. Xú, S., Anwer, N., Mehdi-Souzani, C., Harik, R., Qiao, L.: STEP-NC based reverse engineering of in-process model of NC simulation. *Int J Adv Manuf Technol.* 86, 3267–3288 (2016). <https://doi.org/10.1007/s00170-016-8434-6>
22. Benkő, P., Várady, T.: Segmentation methods for smooth point regions of conventional engineering objects. *Comput Des.* 36, 511–523 (2004). [https://doi.org/10.1016/S0010-4485\(03\)00159-3](https://doi.org/10.1016/S0010-4485(03)00159-3)
23. Jianbing Huang, Chia-Hsiang Menq: Automatic data segmentation for geometric feature extraction from unorganized 3-D coordinate points. *IEEE Trans Robot Autom.* 17, 268–279 (2001). <https://doi.org/10.1109/70.938384>
24. Csákány, P., Wallace, A.M.: Computation of Local Differential Parameters on Irregular Meshes. In: Cipolla, R. and Martin, R. (eds.) *The Mathematics of Surfaces IX*. pp. 19–33. Springer London, London (2000). [https://doi.org/10.1007/978-1-4471-0495-7\\_2](https://doi.org/10.1007/978-1-4471-0495-7_2)
25. Várady, T., Facello, M.A., Terék, Z.: Automatic extraction of surface structures in digital shape reconstruction. *Comput Des.* 39, 379–388 (2007). <https://doi.org/10.1016/j.cad.2007.02.011>
26. Peng, Y.H.; Gao, C.H.; He, B.W.: Research on the relationship between triangle quality and discrete curvature. *China Mech Eng.* 19, 2459–2462, 2468 (2008)
27. Peng, Y., Chen, Y., Huang, B.: Region segmentation for STL triangular mesh of CAD object. *Int J Sens Networks.* 19, 62–68 (2015). <https://doi.org/10.1504/ijnsnet.2015.071383>
28. Hase, V., Bhalerao, Y., Verma, S., Vikhe, G.: Blend recognition from CAD mesh models using pattern matching. *AIP Conference Proceedings* 2148,030029 (2019). <https://doi.org/10.1063/1.5123951>
29. Katz, S., Tal, A.: Hierarchical mesh decomposition using fuzzy clustering and cuts. *ACM Trans Graph.* 22, 954 (2003). <https://doi.org/10.1145/882262.882369>
30. Katz, S., Leifman, G., Tal, A.: Mesh segmentation using feature point and core extraction. *Vis Comput.* 21, 649–658 (2005). <https://doi.org/10.1007/s00371-005-0344-9>

31. Mortara, M., Patané, G., Spagnuolo, M., Falcidieno, B., Rossignac, J.: Blowing Bubbles for Multi-Scale Analysis and Decomposition of Triangle Meshes. *Algorithmica*. 38, 227–248 (2004). <https://doi.org/10.1007/s00453-003-1051-4>
32. Muraleedharan, L.P., Kannan, S.S., Karve, A., Muthuganapathy, R.: Random cutting plane approach for identifying volumetric features in a CAD mesh model. *Comput Graph*. 70, 51–61 (2018). <https://doi.org/10.1016/j.cag.2017.07.025>
33. Shapira, L., Shamir, A., Cohen-Or, D.: Consistent mesh partitioning and skeletonisation using the shape diameter function. *Vis Comput*. 24, 249–259 (2008). <https://doi.org/10.1007/s00371-007-0197-5>
34. Hase, V., Bhalerao, Y., Vikhe Patil, G., Nagarkar, M.: Intelligent Threshold Prediction for Hybrid Mesh Segmentation Through Artificial Neural Network. In: Brijesh I., Deshpande P., Sharma S., Shiurkar U.(eds) *Computing in Engineering and Technology, Advances in Intelligent Systems and Computing 1025*, pp.889-899, Springer.(2019). [https://doi.org/10.1007/978-981-32-9515-5\\_83](https://doi.org/10.1007/978-981-32-9515-5_83)
35. Kim, H.S., Choi, H.K., Lee, K.H.: Feature detection of triangular meshes based on tensor voting theory. *Comput Des*. 41, 47–58 (2009). <https://doi.org/10.1016/j.cad.2008.12.003>
36. Hase, V., Bhalerao, Y., Jadhav, S., Nagarkar, M.: Automatic Interacting Feature Recognition from CAD Mesh Models based on Hybrid Mesh Segmentation. *Int J Adv Manuf Technol*.(Communicated).
37. Hase, V., Bhalerao, Y., Verma, S., Wakchaure, V.: Automatic Interacting Hole Suppression from CAD Mesh Models.. In: Brijesh I., Deshpande P., Sharma S., Shiurkar U.(eds) *Computing in Engineering and Technology, Advances in Intelligent Systems and Computing 1025*, pp.855-865, Springer.(2019).[https://doi.org/10.1007/978-981-32-9515-5\\_80](https://doi.org/10.1007/978-981-32-9515-5_80)
38. Kaick, O.V.A.N., Fish, N.O.A., Kleiman, Y., Asafi, S., Cohen-or, D.: Shape Segmentation by Approximate Convexity Analysis. 34, 1–11 (2014)
39. Hase,V., Bhalerao, Y., Verma, S., Vikhe, G.: Intelligent Systems for Volumetric Feature Recognition from CAD Mesh Models. In: Haldorai A., Ramu A., Mohanram S., Onn C. (eds) *EAI International Conference on Big Data Innovation for Sustainable Cognitive Computing. EAI/Springer Innovations in Communication and Computing*, pp.109-119, Springer. (2018). [https://doi.org/10.1007/978-3-030-19562-5\\_11](https://doi.org/10.1007/978-3-030-19562-5_11)